CENTRAL ASIAN JOURNAL OF THEORETICAL AND APPLIED SCIENCES

Volume: 02 Issue: 02 | February 2021 **ISSN:** 2660-5317

Analyzing Solar Flares using the Tashkent SuperSID Monitor

H.E. Eshquvatov[1,2]*., B. J. Ahmedov[1,3] ., Y.A.Tillayev[1]., U.T.Asatov [2]

[1] Ulugh Beg Astronomical Institute Astronomy 33, Tashkent 100052, Uzbekistan

[2]Tashkent Chemical Technological Institute, 32 Navoi Avenue, Tashkent, Uzbekistan

[3]Tashkent Institute of Irrigation and Agricultural Mechanization Engineers, 39 Kari Niyazov Street, Tashkent 100000 ,Uzbekistan

Received 12nd December 2020, Accepted 25th January 2021, Online 04th February 2021

***Abstract-** We analyse solar flares for different VLF (JJI, Japan, NLK, NML, NPM, USA) transmitters signals. The strongest C-class was detected, on January 28, 2016, at Ulugh Beg Astronomical Institute in Tashkent. Super SID monitor can detect the SID (Sudden Ionospheric Disturbance) due to solar flares by recording the Very Low Frequency (VLF, 3- 30 kHz) signals emitted by transmitters. Sudden Ionospheric Disturbances are the immediate effects of solar flares, which impact the earth and affect the upper atmospheric layers and the system of telecommunication. Summary of the global data from GOES -13 which the local data generated by the receiver used for revealed an unusual spikes in the region of a low Solar flares on January 28, 2016. Solar scientists classified it as an C-flare, in this case an C9.6-class flare. The flare peaked at about 12:02pm. We also analyse Solar flares observed by Tashkent Super SID receiver and show that results are the same with the results of GOES.*

***Keywords-**Very Low Frequency (VLF); Sudden Ionospheric Disturbance (SID); Solar Flares; GOES; AWESOME; SuperSID Monitor.*

INTRODUCTION

The conducting Earth is surrounded by comparatively non conducting atmosphere of thickness 60-80km. The layer above it is the ionosphere extending up to ~ 1000km which is the uppermost part of the atmosphere, distinguished because it is ionized by solar ultraviolet and X-Ray wavelengths radiation. At heights of above 80 km the atmosphere is so thin that free electrons can exist for substantial periods of time before recombining with an ion. The number of these free electrons is sufficient to affect radio wave propagation. The amount of ionization in the ionosphere varies greatly with the amount of radiation received from the Sun depending on diurnal, seasonal effects, the sunspot cycle, and latitude. There are also mechanisms that disturb the ionosphere and decrease the ionization. Free electrons in the ionosphere are able to affect microwave signal's propagation and introduce signal's delay or advance; especially, vulnerable are single-frequency GNSS users. Using GNSS receivers with more frequencies, ionospheric effects can be measured or corrected using at least two different signal frequencies [1,2,6,7,8].

A solar flare is an explosion on the Sun that happens when energy stored in twisted magnetic fields (usually above sunspots) is suddenly released. Flares produce a burst of radiation across the electromagnetic spectrum. Solar flares are classified according to their X-ray brightness in the wavelength range 0.1-0.8nm. There are 3 categories: X-class flares are big; they are major events that can trigger planet-wide radio blackouts and long-lasting radiation storms. M-class flares are medium-sized; they can cause brief radio blackouts that affect Earth's polar regions. Minor radiation storms sometimes follow an M-class flare. C-class flares are small with few noticeable consequences here on Earth. Each category for X-ray flares has nine sub divisions ranging from 1 to 9 [9,10,11].

The solar are classes are shown in table 1. When solar flares occur the X-radiation with wavelengths less than 1 nm increases in strength so as to produce increased ionization in the D layer of the ionosphere at heights around 80km. The increase in electron concentration leads to several phenomena grouped together under the name sudden ionospheric disturbance (SID). As described earlier, the disturbance has a profound effect on the travel of radio waves. Because SIDs are produced by photon radiation from the Sun they occur only on the sunlit side of the Earth and their effects are most intense when the Sun is near the zenith. During an SID the electron content of the D layer increases very suddenly within a few minutes and afterwards slowly recovers to its normal magnitude within 0.75 - 1.5 hours [3].

Table 1: The solar flare classes and their associated peak fluxes

Solar Flare Classes	Peak between 0.1-0.8nm [Watts/m^2]
A	$< 10^{-7}$
B	10^{-7}-10^{-6}
C	10^{-6}-10^{-5}
M	10^{-5}-10^{-4}
X	$> 10^{-4}$

2. Operations and Methods

The type of antenna that can pick up VLF radio signals is called a loop antenna. Fundamentally, a loop antenna is an LC (inductor capacitor) circuit which resonates at some frequency. An inductor concentrates and stores magnetic energy, while a capacitor concentrates charge and thereby stores electric energy. The inductance is formed by the wire loop. The capacitance is formed by the wiring metal surface, running in parallel along the loop. Wire resistance is small, though always present in a wire and increases as the length of the wire increases. As the electromagnetic field from a VLF station passes by the loop, a very small (~ 0.1 mV) electrical current is induced in the wire.

To obtain better signal, one can either increase the number of turns of the wire loop or enlarge the size of the antenna. As the number of turns increases, the distributed capacitance also increases, which lowers the resonant frequency. Also, when the number of turns increases, the resistance of the wire increases too, causing the amplitude of the signal to drop. Fortunately, electronic amplifiers can magnify small signals hundreds or thousands of times. In order to measure and study sudden ionospheric disturbances (SIDs), I have built a wire loop antenna myself. The assembly parts, including hardware and software, were provided by Stanford Solar Centre.

The antenna with the assigned name UBAI is situated at Ulugh Beg Astronomical Institute at the 38 room in Tashkent. The insulated copper wire is wound around a 2 m square wooden frame about 30 times. The frame acts as a support for the wire and is screwed on to the wooden wall. The two ends of the wire are connected (via terminal block) to the 9 m coaxial cable, which travels to the control room, see figures 1,2,3.

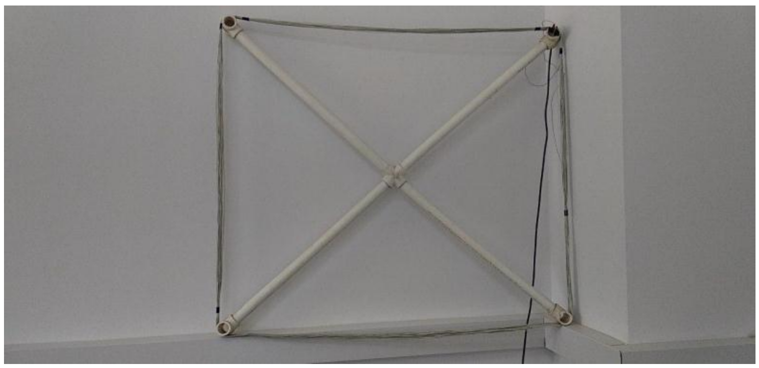

Fig.1 The antenna assembly at Astronomical Institute in Tashkent. The wire is wound around a 2 m square wooden frame about 30 times.

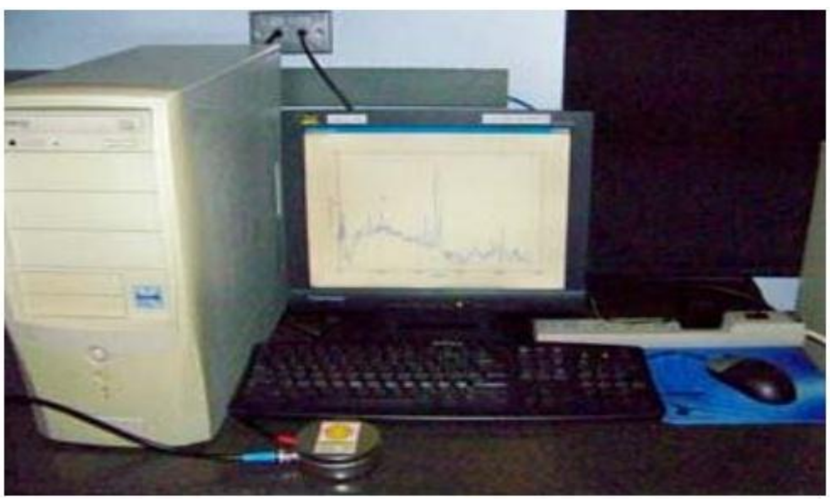

Fig.2 SuperSID preamp. Temporarily set up your antenna near your SID and computer.

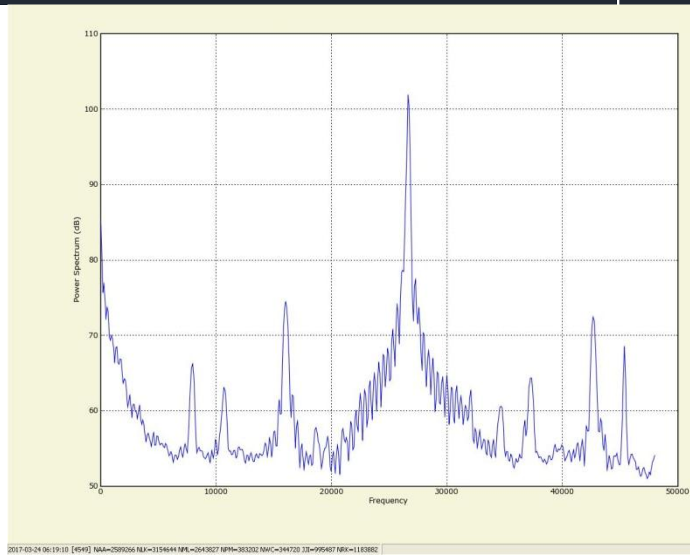

Fig.3 Results for SuperSID monitor.

3. Results and Discussion

Measuring sudden ionospheric disturbances successfully at Ulugh Beg Astronomical Institute for January 28, 2016, the strongest solar flare C9.6 and the weakest C5.3 have been classified. The strongest C-classes are detected, on January 28, 2016 at Tashkent. The table 2 shows a list of narrow band transmitters commonly recorded by Atmospheric Weather Electromagnetic System for Observation Modeling and Education (AWESOME), though it should be noted that transmitters do, so this list may change. The instruments and data have been shown to be appropriate to, and usable by, high school age and early university students. Data contributed to the Stanford data center is openly shared and partnerships between groups in different nations develop naturally. Students and teachers have direct access to scientific expertise. The result is a world-wide collaboration of scientists, teachers, and students to investigate the variability of the ionosphere. The research-quality AWESOME (Atmospheric Weather Electromagnetic System of Observation Modeling and Education) instruments have been selected as a participating program by the United Nations Basic Space Science Initiative (UNBSSI) Fig.5. D-region ionospheric perturbation caused by the astrophysical and geophysical phenomena such as Solar Flares, lightning induced electron precipitations, cosmic gamma ray flares, terrestrial gamma rays flares, geomagnetic storm effect, etc.[4,5].

Table 2: The list of narrowband transmitters commonly recorded by AWESOME

LAT	**LON**	**FREQ**	**SIGN**	**LOCATION**	**FORMAT**	**kW**
8.47	77.40	18200Hz	VTX	Katabomman, India	FSK	
40.70	1.25	18300Hz	HWU	Rosnay, France	MSK 4	400

52.71	3.07	19600Hz	GBZ	Anthorn, Great Britain (NATO)	FSK	30
-21.80	114.20	19800Hz	NWC	North West Cape, Australia (USA)	MSK	1000
40.88	9.68	20270Hz	ICV	Isola di Tavolara, Italy (NATO)	MSK	20
40.70	1.25	20900Hz	HWU	Rosnay, France	MSK 4	400
20.40	-158.20	21400Hz	NPM	Lualualei, Hawaii, USA	MSK	424
40.70	1.25	21750Hz	HWV	Le Blanc, France (NATO)	MSK	200
52.40	-1.20	22100Hz	GQD	Anthorn, Great Britain (NATO)	FSK	52.40
32.04	130.81	22200Hz	JJI	Ebino, Japan	FSK	200
53.10	7.60	23400Hz	DHO	Rhauderfehn, Germany	FSK	800
44.65	-67.30	24000Hz	NAA	Cutler, Maine, USA	MSK	1000
48.20	-121.90	24800Hz	NLK	Jim Creek, Washington, USA	MSK	192
46.35	-98.33	25200Hz	NLM	LaMoure, North Dakota, USA	MSK	
37.43	27.55	26700Hz	TBB	Bafa, Turkey	MSK	
65.00	-18.00	37500Hz	NRK	Grindavik, Iceland (USA)	MSK	
18.00	-67.00	40750Hz	NAU	Aguado, Puerto Rico (USA)	MSK	100
38.00	13.50	45900Hz	NSC	Sicily, Italy (USA)	MSK	

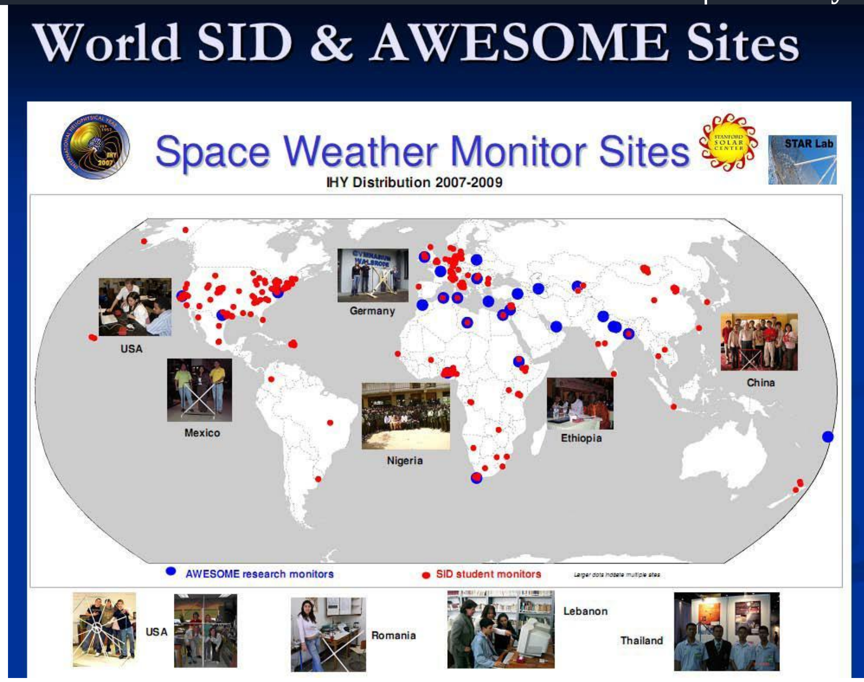

Fig.5 Map for Tashkent VLF station and Tashkent Super SID monitor. Blue circles indicates the position of Tashkent VLF station, red circles indicates the positions of Super SID monitor.

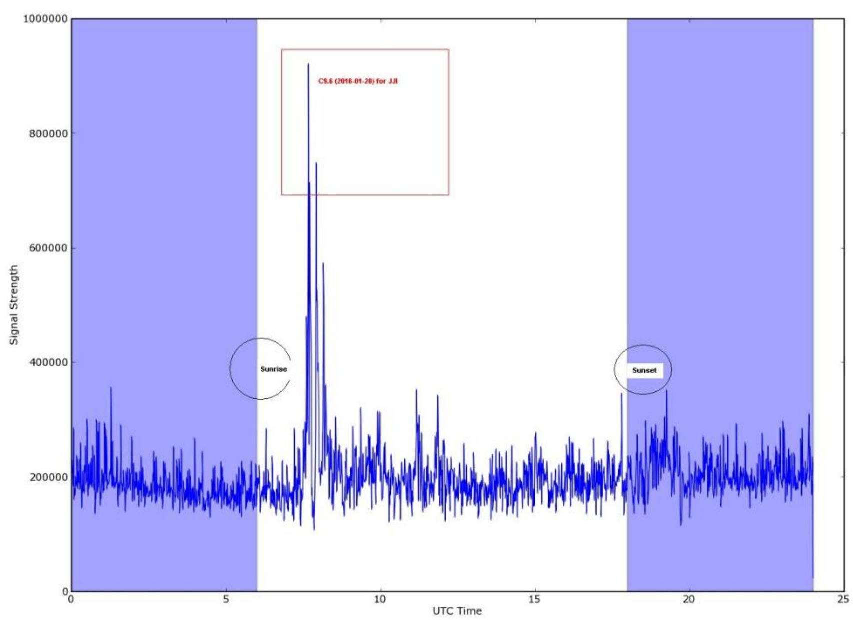

Fig.6 The figure shows recent solar flare (Jan 28, 2016), which was obtained at Tashkent site. Red square represent area where the coinciding flare for JJJ transmitter signal occur. Black circles denote sunrise and sunset.

CENTRAL ASIAN JOURNAL OF THEORETICAL AND APPLIED SCIENCES
Volume: 02 Issue: 02 | February 2021, ISSN: 2660-5317

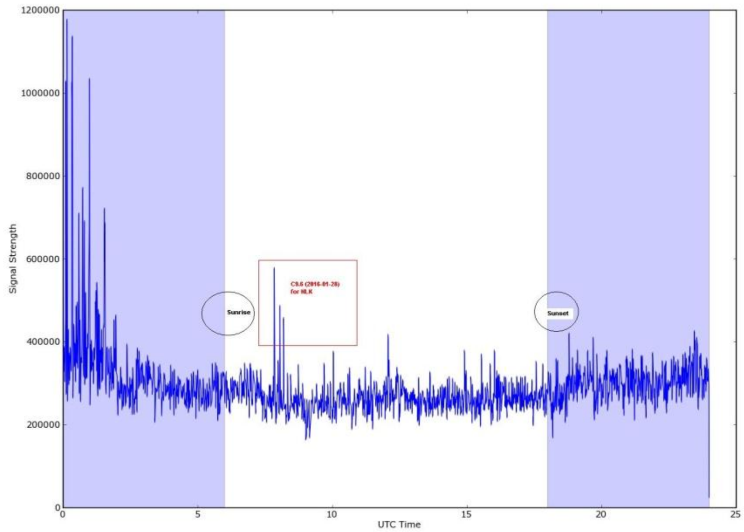

Fig.7 The figure shows recent solar flare (Jan 28, 2016), which was obtained at Tashkent site. Red square represent area where the coinciding flare for NLK transmitter signal occur. Black circles denote sunrise and sunset.

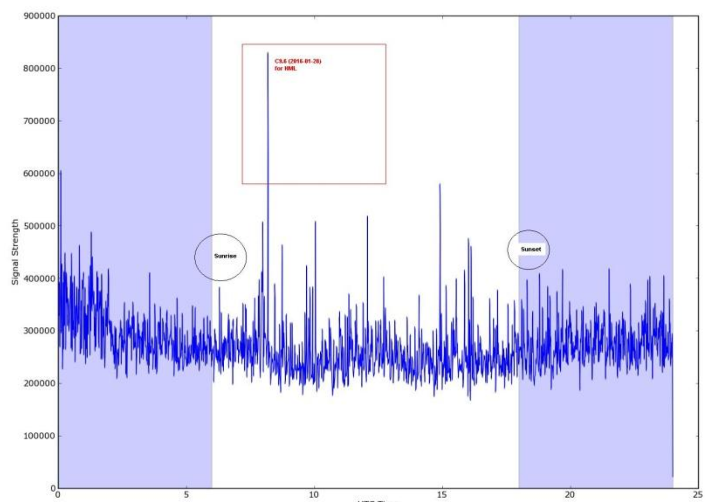

Fig.8 The figure shows recent solar flare (Jan 28, 2016), which was obtained at Tashkent site. Red square represent area where the coinciding flare for NML transmitter signal occur. Black circles denote sunrise and sunset.

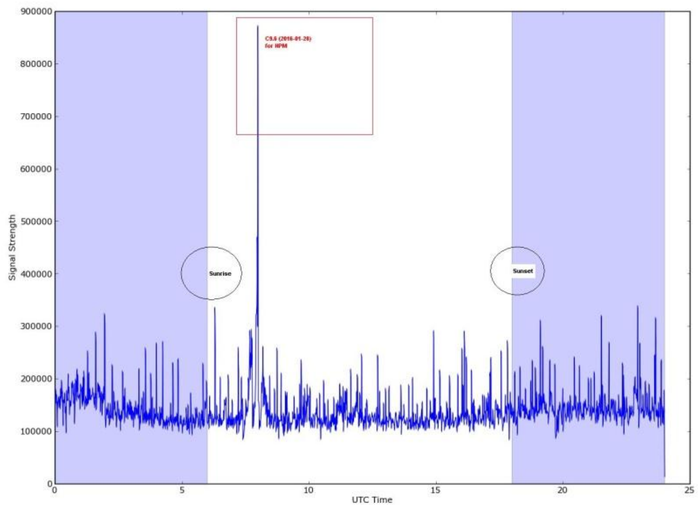

Fig.9 The figure shows recent solar flare (Jan 28, 2016), which was obtained at Tashkent site. Red square represent area where the coinciding flare for NPM transmitter signal occur. Black circles denote sunrise and sunset.

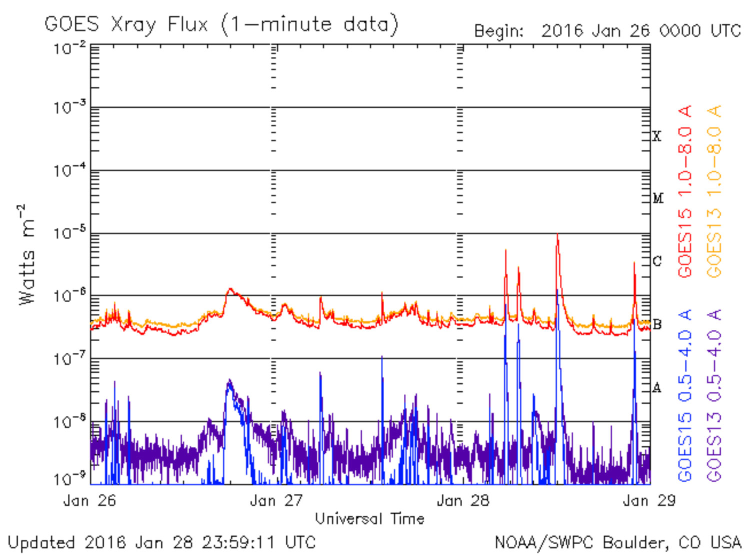

Fig10 The figure shows recent solar flares during 26-28 January 2016.

4. Conclusion

I this study, we detection of C-class solar flares were analysed that occurred during daytime, considering the local time of the monitor at Tashkent SuperSID receiver. Solar flares (January 28, 2016) observed by Tashkent Super SID receiver are shown in Figs. 6-9. Red squares represent areas where the coinciding flares for different VLF (JJI, Japan, NLK, NML, NPM, USA) transmitter signals occur. Black circles denote sunrise and sunset, where the signal strength suddenly drops or rises. Figures 6-9 show an overall good agreement between the observed activities on the Sun , conditions in the ionosphere, Tashkent SuperSID-derived data . As can be seen from Figures 6-9 our result is in agreement with the results of GOES illustrated in Fig.10.

Acknowledgment

This research is supported in part by Projects No. VA-FAF-2-008, No. MRB-AN-2019-29 and FA-Atech-2018-392 of the Uzbekistan Ministry for Innovative Development, by the Abdus Salam International Centre for Theoretical Physics under the Office of External Activities.

References

1. Ahmedov, B.J., Tojiev, S.R., Eshkuvatov H.E. Total Electron Content (TEC) Extraction using Kitab and Tashkent GPS stations. **Uzbek Journal of Physics**, №6,.pp361-366, 2016.
2. Ahmedov, B.J., Tojiev, S.R., Eshkuvatov H.E. Low radiofrequency radiation in the D-layer of the ionosphere and possibility of their registration on Tashkent VLF station. **Uzbek Journal of Physics**, Vol.17,№6, pp.339-350, 2015 .
3. Ratcliffe J.A.: An introduction to the ionosphere and magnetosphere. Cambridge University Press, 1972, ISBN 0-521-08341-9.
4. Barr, R., D. Llanwyn Jones, and C. J. Rodger. "ELF and VLF radio waves. **Journal of Atmospheric and Solar- Terrestrial Physics,** 62.17, 1689-1718, 2000.
5. Pal, Sujay: Numerical modelling of VLF radio wave propagation through earth-ionosphere waveguide and its application to sudden ionospheric disturbances. March 2015, 150pp, arXiv:1503.05789.
6. Tojiev, S.R., Ahmedov, B.J., Tillayev, Y.A., Eshkuvatov, H.E. Ionospheric anomalies of local earthquakes detected by GPS TEC measurements using data from Tashkent and Kitab stations. **Advances in Space Research**, 52, 1146–1154, 2013.
7. Tojiev, S.R., Ahmedov, B.J., Eshkuvatov H.E., Ionospheric pecursors of earthquakes recorded by VLF receiver at Tashkent IHY station, **Advances in Space Research**, Vol.54,pp.628-643, 2014.
8. Tojiev, S.R., Morozova, V.S., Ahmedov, B.J., Eshkuvatov, H.E. Electromagnetic studies of ionospheric and magnetospheric perturbations associated with the earth, atmospheric and astrophysical phenomena. In: Camci, U., Semiz, I. (Eds.), Mathematical Physics. World Scientific, pp. 254–278, 2012.
9. Mansilla G.A. Ionospheric Storm Effects at the Equatorial Anomaly. **International Journal of Geomagnetism and Aeronomy**. 4(3): 209-214, 2003.
10. Hayakawa, M., Molchanov, O.A. (Eds.). Seismo Electromagnetics Lithosphere–Atmosphere–Ionosphere Coupling. TERRAPUB, Tokyo, p. 477, 2002.
11. Francisca D., Macalalad E., Vallar E., Galvez M.C., Tsai L. C. and Hsiao T.Y. VHF/UHF amplitude scintillation observed by the low-latitude ionospheric tomography network (LITN). **ARPN Journal of Engineering and Applied Sciences**. 10(22): 10324- 10327, 2015.

